Double Path Interference and Magnetic Oscillations in Cooper Pair Transport through a Single Nanowire

Sergei V. Mironov, Alexandre S. Mel'Nikov, Alexandre I. Buzdin

Double Path Interference and Magnetic Oscillations in Cooper Pair Transport through a Single Nanowire

S. V. Mironov,[1,2] A. S. Mel'nikov,[2,3] and A. I. Buzdin[1]
[1]University Bordeaux, LOMA UMR-CNRS 5798, F-33405 Talence Cedex, France
[2]Institute for Physics of Microstructures, Russian Academy of Sciences, 603950 Nizhny Novgorod GSP-105, Russia
[3]Lobachevsky State University of Nizhny Novgorod, 23 Gagarina, 603950 Nizhny Novgorod, Russia
(Received 6 November 2014; published 2 June 2015)

We show that the critical current of the Josephson junction consisting of superconducting electrodes coupled through a nanowire with two conductive channels can reveal the multiperiodic magnetic oscillations. The multiperiodicity originates from the quantum mechanical interference between the channels affected by both the strong spin-orbit coupling and the Zeeman interaction. This minimal two-channel model is shown to explain the complicated interference phenomena observed recently in Josephson transport through Bi nanowires.

DOI: 10.1103/PhysRevLett.114.227001 PACS numbers: 74.45.+c, 73.63.Nm, 74.78.Na

The systems with a few conductive channels provide a unique possibility for constructing nanoelectronic devices with tunable transport properties at the quantum length scale. One of the promising realizations of these devices is based on the localized electronic states appearing, for example, at the surface of topological insulators [1], at the edges of graphene nanoribbons [2], and in InAs, InSb, and Bi nanowires [3–6]. The physics of the charge transport through these states appears to be extremely rich due to strong spin-orbit coupling, large anisotropic g-factors, etc. The unique normal state properties naturally also cause unusual proximity phenomena revealing themselves for the edge states coupled to the bulk superconducting leads [1,3]. Such a coupling provides a possibility for constructing new types of Josephson devices where an external magnetic field H can effectively control the current-phase relation [7,8] and provide favorable conditions for the appearance of Majorana fermions [9–11].

In this Letter we provide a theoretical description of the magnetotransport phenomena in a Josephson system containing a few conductive channels which model the edge states localized, e.g., at the surface of a single nanowire (see Fig. 1). Specifically, we propose a generic model accounting for only two interfering electron paths or conductive channels and strong spin-orbit and Zeeman interactions. This model allows us to describe both orbital and spin mechanisms of the magnetic field effect and to uncover the microscopical mechanisms responsible for the formation of the nontrivial ground state of the Josephson junction with a nonzero superconducting phase difference. The Zeeman interaction produces the spatial oscillation of the Cooper pair wave function at the scale $\hbar v_F/g\mu_B H$ (similar to the ones in superconductor-ferromagnet structures [7]) which results in the magnetic oscillations of the critical current with the period $\hbar v_F/g\mu_B L$, where L is the channel length. The orbital effect causes a standard phase gain $\sim 2\pi HS/\Phi_0$ ($\Phi_0 = \pi\hbar c/|e|$ is the flux quantum) in the electronic wave function similar to the one appearing in the Aharonov-Bohm (AB) effect. Here S is the area enclosed by the pair of interfering paths projected on the plane perpendicular to the magnetic field. The interfering quantum mechanical amplitudes in this case cause the magnetic oscillations in the total transmission amplitude with the period $2\Phi_0/S$. The Andreev reflection at the superconducting boundaries can double the effective charge in the oscillation period [12], and we show that, in the general case, the resulting critical current oscillates with the competing periods $2\Phi_0/S$ and Φ_0/S.

The above physical picture should, of course, be modified in the presence of the spin-orbit coupling which can produce the spontaneous Josephson phase difference φ_0 [8]. Despite the fact that this anomalous Josephson effect was found within several different theoretical models [13–19], its microscopical origin still remains disputable. We clarify this question and show that the key ingredient for the φ_0-junction formation is the nonparabolicity of the electron energy spectrum, which in the presence of spin-orbit coupling gives rise to the dependence of the Fermi velocity on momentum direction. Under the influence of the Zeeman field, such specific dependence results in the spontaneous Josephson ground state phase φ_0 and in the renormalization of the above magnetic oscillation periods.

Turning to the existing experimental data, we must note that the multiperiodic magnetic oscillations have recently been observed in measurements of the Josephson critical

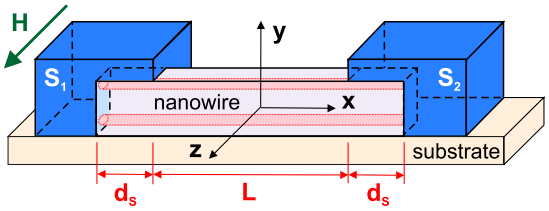

FIG. 1 (color online). A model Josephson junction with a two-channel nanowire in an external magnetic field.

current through the Bi nanowires [20]. Such wires are known to reveal the unusual combination of properties mentioned above: (i) strong Rashba spin-orbit coupling with the energy comparable to the Fermi energy [21,22], (ii) large g-factor $\sim 10^2$ for certain directions of the magnetic field [23], (iii) large Fermi wavelength $\lambda_F \sim 50$ nm [24], which makes it easy to create nearly one-dimensional wires. As we show below, our model can provide a simple fit of the oscillatory behavior discovered in Ref. [20], being, thus, a promising candidate for the description of the interference physics in such systems.

Our calculation of the critical current of the two-channel nanowire is based on the Bogoliubov–de Gennes (BdG) approach, and the setup is shown in Fig. 1. The current-phase relation of the Josephson junction is defined by the dependence of the quasiparticle excitation energies ε on the Josephson phase φ (we put $\hbar = 1$) [25]:

$$I(\varphi) = -2e \sum_{\varepsilon \in (0;\infty)} \frac{\partial \varepsilon}{\partial \varphi} \tanh\left(\frac{\varepsilon}{2T}\right), \tag{1}$$

where ε should be found from the BdG equations

$$\begin{pmatrix} \hat{H} & \hat{\Delta} \\ \hat{\Delta}^\dagger & -\hat{H}^\dagger \end{pmatrix} \begin{pmatrix} u \\ v \end{pmatrix} = \varepsilon \begin{pmatrix} u \\ v \end{pmatrix}. \tag{2}$$

The electron- and holelike parts of the quasiparticle wave function u and v are multicomponent: $u = (u_{1\uparrow}, u_{2\uparrow}, u_{1\downarrow}, u_{2\downarrow})$ and $v = (v_{1\uparrow}, v_{2\uparrow}, v_{1\downarrow}, v_{2\downarrow})$, where the first indices enumerate the conductive channels and arrows indicate the z-axis spin projections. In Eq. (2) $\hat{\Delta}$ is the superconducting proximity induced gap and $\hat{H}$ is the single-electron (4×4)-matrix Hamiltonian of the isolated wire, which for zero magnetic field takes the form

$$\hat{H} = [\xi(\hat{p}) - \mu + \alpha \hat{p} \hat{\sigma}_z] \otimes \hat{I} + \hat{V}(x). \tag{3}$$

Here $\hat{p} = -i\partial_x$ is the momentum along the x axis, $\xi(p)$ is the electron energy in the isolated wire, μ is the chemical potential, the term $\alpha \hat{p} \hat{\sigma}_z$ describes the Rashba spin-orbit coupling due to the broken inversion symmetry in the y direction [26], $\hat{I}$ is a 2×2 unit matrix in the channel subspace, and the potential $\hat{V}(x)$ describes the scattering at the S-nanowire interfaces. Applying the magnetic field we should include the Zeeman term $g\mu_B H \hat{\sigma}_z$ into Eq. (3) and replace $\hat{p}$ with $(\hat{p} + |e|A_x/c)$, where $A_x(y) = -Hy$. We intentionally choose the direction of the magnetic field which assumes the absence of the mixing of spin bands and the resulting Majorana states [27–29] to focus on the study of interference effects relevant to the experiment [20].

Our strategy is to find the quasiclassical solutions of Eq. (2) inside the nanowire where both $\hat{\Delta}$ and $\hat{V}$ are zero and to match the solutions at the ends of the wire using phenomenological scattering matrices. As a first step we derive the quasiclassical version of Eq. (2) inside the wire. Taking, e.g., the functions $u_{1\uparrow}$ and $u_{2\uparrow}$, one can separate the fast oscillating exponential factor: $u_{n\uparrow} = \tilde{u}^{\pm}_{n\uparrow} e^{\pm i p_F^{\pm} x}$, where the Fermi momenta p_F^+ and p_F^- for $p > 0$ and $p < 0$ are different in the presence of the spin-orbit coupling. Then, from the BdG equation (2) with $\hat{\Delta} = 0$, $\hat{V} = 0$, and $H = 0$, we find

$$[\xi(p_F^{\pm}) - \mu \pm \alpha p_F^{\pm}] \tilde{u}^{\pm}_{n\uparrow} \mp i[\xi'(p_F^{\pm}) \pm \alpha] \partial_x \tilde{u}^{\pm}_{n\uparrow} = \varepsilon \tilde{u}^{\pm}_{n\uparrow}, \tag{4}$$

where $\xi'(p) \equiv \partial \xi / \partial p$. The Fermi momenta are defined by the equations $\xi(p_F^{\pm}) = \mu \mp \alpha p_F^{\pm}$. Assuming α to be small, we find $p_F^{\pm} \approx [1 \mp \alpha/\xi'(p_F^0)] p_F^0$, with $\xi(p_F^0) = \mu$, and obtain

$$\mp i v_F^{\pm} \partial_x \tilde{u}^{\pm}_{n\uparrow} = \varepsilon \tilde{u}^{\pm}_{n\uparrow}. \tag{5}$$

The derivation of equations for $u^{\pm}_{n\downarrow}$, $v^{\pm}_{n\uparrow}$, and $v^{\pm}_{n\downarrow}$ [30] is straightforward. Using the expansion $\xi'(p_F^{\pm}) = \xi'(p_F^0) \mp \alpha p_F^0 \xi''(p_F^0)/\xi'(p_F^0)$, we find the Fermi velocities:

$$v_F^{\pm} = \xi'(p_F^0) \pm \alpha [1 - p_F^0 \xi''(p_F^0)/\xi'(p_F^0)]. \tag{6}$$

Clearly the spin-orbit coupling results in the difference between the Fermi velocities v_F^+ and v_F^- of quasiparticles with opposite momenta. This renormalization (6) is absent only for the exactly quadratic spectrum. It is the difference between v_F^+ and v_F^- which is responsible for the so-called φ_0-junction formation (see Ref. [8] and the discussion below). Thus, the above derivation explains the results of Ref. [31], where no φ_0-junction was found for the $\xi(p) \propto p^2$ spectrum, and the subsequent misinterpretation for the conditions of the φ_0-junction emergence in Ref. [32]. Note that another possibility to get the φ_0-junction even for the quadratic electron spectrum is to consider nonballistic two-dimensional quasiparticle motion [19].

Introducing the four-component envelope wave functions $w_\sigma^{\pm}(x) = (\sqrt{v_F^{\pm}} \tilde{u}^{\pm}_{1\sigma}, \sqrt{v_F^{\pm}} \tilde{u}^{\pm}_{2\sigma}, \sqrt{v_F^{\mp}} \tilde{v}^{\mp}_{1-\sigma}, \sqrt{v_F^{\mp}} \tilde{v}^{\mp}_{2-\sigma})$ and neglecting the spin flip at the wire ends, we can write the matching conditions, e.g., for $w_\uparrow^{\pm}$: $w_\uparrow^{\pm}(\pm L/2) = \hat{T}^{\pm} w_\uparrow^{\pm}(\mp L/2)$ and $w_\uparrow^{\mp}(\pm L/2) = \hat{Q}^{\pm} w_\uparrow^{\pm}(\pm L/2)$, where L is the wire length, the unitary matrices $\hat{T}^{\pm}$ and $\hat{Q}^{\pm}$ describe the quasiparticle transmission along the wire, and there is both normal and Andreev scattering at the wire ends. The solvability condition $\det[\hat{Q}^- \hat{T}^- \hat{Q}^+ \hat{T}^+ - \hat{1}] = 0$ [25,33] for the above matching equations defines the quasiparticle energy spectrum ε. Replacing α and g by $-\alpha$ and $-g$, one finds ε for the opposite spin component.

The general form of the matrices $\hat{T}^{\pm}$ and $\hat{Q}^{\pm}$ is

$$\hat{T}^{\pm} = \begin{pmatrix} e^{i p_F^{\pm} L} \hat{M}^{\pm} & \hat{0} \\ \hat{0} & e^{-i p_F^{\mp} L} \hat{M}^{\mp} \end{pmatrix}, \quad \hat{Q}^{\pm} = \begin{pmatrix} \hat{R}_e^{\pm} & \hat{A}_h^{\mp} \\ \hat{A}_e^{\pm} & \hat{R}_h^{\mp} \end{pmatrix}. \tag{7}$$

The 2×2 matrices $\hat{M}^{\pm}$ are defined from the solution of Eq. (5) under the assumption of different g-factors g_1 and g_2 in different channels: $\hat{M}^{\pm}_{nl} = \exp[iq^{\pm} L \mp (-1)^n i\pi\phi/2] \delta_{nl}$, where $\phi = HLD/\Phi_0$ is the dimensionless magnetic flux

(the channels pass along the plane $y = \pm D/2$), $q^{\pm} = (\varepsilon - g_n\mu_B H)/v_F^{\pm}$, and δ_{nl} is the Kronecker delta. The phenomenological 2×2 matrices $\hat{R}^{\pm}_{e(h)}$ and $\hat{A}^{\pm}_{e(h)}$ describe the normal and Andreev reflection from the S leads, respectively [34].

First, we consider the limit when the quasiparticles experience *full* Andreev reflection in each channel separately. We assume that such an Andreev reflection is caused by the superconducting gap Δ_n induced in the n-th channel due to the proximity effect on the S leads. In the case when the S leads cover the ending parts of the nanowire, the asymmetry in the relative position between the channels and the superconductor can result in $\Delta_1 \neq \Delta_2$. The specific values for Δ_n strongly depend on the microscopical properties of S-nanowire interfaces and hereafter we consider Δ_n to be the phenomenological parameters [35–39]. The above assumption of the full Andreev reflection means that the size d_s of the induced gap regions (see Fig. 1) well exceeds the relevant coherence length. In this limiting case, the normal scattering vanishes ($\hat{R}^{\pm}_e = \hat{R}^{\pm}_h = \hat{0}$) while the Andreev scattering is described by the matrices $(\hat{A}^{\pm}_e)_{nl} = \delta_{nl} \exp[\mp i\varphi/2 - i \arccos(\varepsilon/\Delta_n)]$. Note that for high tunneling rates between the S leads and the conductive channels, the quasiparticles reveal Andreev reflection inside the bulk S leads. In our model this situation corresponds to $\Delta_1 = \Delta_2 = \Delta_s$ (Δ_s is the gap in the S leads).

In the short junction limit ($\varepsilon L/v_F^{\pm} \ll 1$), only the subgap Andreev states contribute to the Josephson current. Taking into account all of the spin projections, we obtain four positive subgap energy levels:

$$\varepsilon = \Delta_n |\cos[\varphi/2 - (-1)^n \pi\phi/2 \pm g_n\mu_B HL/v_F^{\pm}]|, \quad (8)$$

where n enumerates the channels. For large temperatures $T \gg \Delta_n$ the current-phase relation (1) takes the form

$$I = \sum_{n=1,2} I_n \sin[\varphi + \beta_n H + (-1)^n \pi\phi] \cos(\gamma_n H). \quad (9)$$

Here $I_n = |e|\Delta_n^2/4T$ is the critical current of the nth channel at $H = 0$, the flux ϕ produces the oscillations of I_c similar to the ones in the superconducting quantum interference device (SQUID), and the cosine term depending on the constants $\gamma_n = g_n\mu_B L(1/v_F^{+} + 1/v_F^{-})$ describes the oscillatory behavior of I_c due to the Zeeman interaction similar to the one in superconductor-ferromagnet-superconductor structures [7]. The term $\beta_n H = g_n\mu_B LH(1/v_F^{+} - 1/v_F^{-})$ describes the φ_0-junction formation due to the spin-orbit coupling [8]. The critical current corresponding to Eq. (9) reads

$$I_c^2 = I_1^2\cos^2(\gamma_1 H) + I_2^2\cos^2(\gamma_2 H) + 2I_1 I_2 \cos(\gamma_1 H)\cos(\gamma_2 H)\cos[2\pi\phi + (\beta_1 - \beta_2)H]. \quad (10)$$

Interestingly, if $g_1 \neq g_2$ the spin-orbit coupling influences the period of the SQUID-like orbital oscillations in $I_c(H)$, i.e., renormalizes the effective quantization area enclosed by the channels, $S_{\text{eff}} = LD + \Phi_0(\beta_1 - \beta_2)/2\pi$. Choosing the parameters relevant to the experimental situation in Ref. [20], we obtain a variety of $I_c(H)$ dependencies shown in Fig. 2. These dependencies reproduce not only multiperiodic oscillations due to the interplay of the orbital and Zeeman interactions observed in Ref. [20], but also asymmetry in the form of the upper and lower envelopes. In Figs. 2(a) and 2(b), one can clearly see two periods of oscillations: $\delta H_{\text{orb}} = \Phi_0/S_{\text{eff}}$ and $\delta H_{\text{Zeem}} = 2\pi/\gamma_1 = 2\pi/\gamma_2$. The slow drift of the average current in Fig. 2(d) should be considered, in fact, as a fragment of the large-period oscillations caused by the difference between γ_1 and γ_2. Note that the period δH_{orb} should be sensitive to the tilt of magnetic field in the yz plane, which allows us to distinguish it experimentally from the period δH_{Zeem}.

Now let us study the crossover between the limits of large and small Andreev reflection which occurs with the decrease in the induced gap value. For simplicity we neglect the spin-orbit and Zeeman interactions as well as the difference between the induced gaps ($\Delta_1 = \Delta_2 \equiv \Delta_0$). We assume the interchannel electron transfer to be the only normal scattering mechanism at the wire ends (in the opposite limit of the vanishing interchannel transfer, the current-phase relation should be similar to the one for a quantum box studied in Ref. [40]). Thus, we take $(\hat{R}^{\pm}_{e,h})_{nl} = t(1 - \delta_{nl})$ and $(\hat{A}^{\pm}_{e,h})_{nl} = a\delta_{nl}e^{\mp i\varphi/2}$, where $a = -i\Delta_0 \sinh(qd_s)/Z$, $q = \sqrt{\Delta_0^2 - \varepsilon^2}/v_F$, $t = qv_F/Z$, and $Z = qv_F\cosh(qd_s) + i\varepsilon\sinh(qd_s)$ [41]. The interchannel hopping with the amplitude t allows the formation of closed electron orbits of nonzero area and, thus, can strongly affect the electron transfer through the nanowire due to the interference between the channels. Such a model provides the simplest way to clarify whether these closed orbits can cause the interplay between the $2\Phi_0$ and Φ_0 flux periodicities in the critical current corresponding to the AB interference of electrons and Cooper pairs.

In Fig. 3 we present the results of the critical current calculations for the energy spectrum (see Ref. [42] for

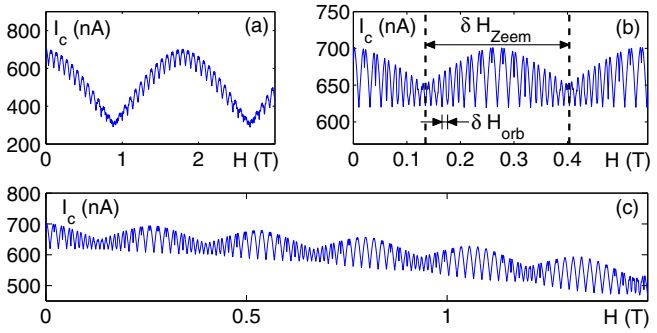

FIG. 2 (color online). The critical current I_c vs the magnetic field H. We choose $T = 0.1$ K, $\Delta_1 = 7.5$ K, $\Delta_2 = 1$ K, $v_F = 3 \times 10^5$ m/s, $L = 2$ μm, and (a) $D = 15$ nm and (b), (c) $D = 50$ nm. We also take (a) $g_1 = g_2 = 1.5$, (b) $g1 = 0$ and $g_2 = 10$, (c) $g1 = 1$ and $g_2 = 10$.

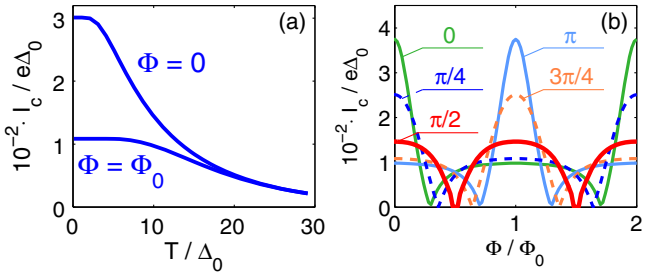

FIG. 3 (color online). (a) The temperature crossover from the $2\Phi_0$-periodic to the Φ_0-periodic oscillation of the critical current I_c. The curves correspond to $\Phi = 0$ and $\Phi = \Phi_0$. We take $L = d_s = 0.01 v_F/\Delta_0$ and $p_F L_0 = \pi/4 + 2\pi m$ (m is an integer number). (b) Dependencies $I_c(\Phi)$ for $T/\Delta_0 = 5$ and $p_F L_0 = \eta + 2\pi m$, where the values η are shown near the curves.

details). The period of $I_c(H)$ oscillations strongly depends on both temperature T and the parameter $p_F L_0 = 2p_F(L + 2d_s)$. This parameter can be different in different samples, resulting in the quasiparticle energy spectrum and Josephson current which fluctuate from sample to sample (mesoscopic fluctuations). In the limit $d_s \gg v_F/\Delta_0$, we get the case of independent channels considered above and restore the Φ_0 periodicity of the $I_c(H)$ oscillations. A substantial difference between the curves $I_c(T)$ for $\Phi = 0$ and $\Phi = \Phi_0$ appears only for $d_s < v_F/\Delta_0$ (this limit is easily achievable since the induced gap Δ_0 can be much smaller than the gap Δ_s in the bulk of the S leads). In this regime the Andreev reflection is weak and one can clearly see the $\Phi_0 - 2\Phi_0$ crossover. For low temperatures $T < v_F/L_0$, the curves in Fig. 3 are strongly different since the system transparency and the corresponding critical current oscillate with the electron AB period $2\Phi_0$. For higher temperatures, the normal metal coherence length v_F/T can become less than the length L_0 of the closed electron path and the $2\Phi_0$-periodic interference of electrons cannot contribute to the superflow through the junction. Thus, with the temperature increase ($T > v_F/L_0$), the difference between curves in Fig. 3 vanishes and I_c oscillates with the AB period of the Cooper pairs (Φ_0). Note that for $p_F L_0 = \pi/2$, the energy spectrum reveals the symmetry $\varepsilon(\Phi + \Phi_0, \varphi + \pi) = \varepsilon(\Phi, \varphi)$ [42] and, thus, the $I_c(H)$ oscillations have the period Φ_0 for all temperatures.

At temperatures close to T_c, it is natural to expect that the system behavior can be described by the Ginzburg-Landau model modified to include the Zeeman and spin-orbit interactions. Keeping only the terms of the order $O(\Psi^2)$, we consider the free energy F in the form [43,44]

$$F = \sum_{n=1,2} \int \{a|\Psi_n|^2 + \gamma|\hat{D}_x\Psi_n|^2 + \beta|\hat{D}_x^2\Psi_n|^2 - \nu H[\Psi_n(\hat{D}_x\Psi_n)^* + \Psi_n^*(\hat{D}_x\Psi_n)]\}dx, \quad (11)$$

where Ψ_n is the superconducting order parameter in the n-th channel, $a(x) \sim [T - T_c(x)]$, and, inside the wire $a > 0$, $\hat{D}_x = -i\partial_x + 2\pi A_x/\Phi_0$ and the constant $\nu \sim \alpha g$ describes the strength of the spin-orbit coupling. The oscillatory behavior of Ψ_n due to the Zeeman interaction reveals only for the magnetic fields above the tricritical Lifshitz point, i.e., for $\gamma < 0$ [7]. Accounting for the higher order gradient term with $\beta > 0$ in Eq. (11), one finds an additional characteristic length scale $\xi_f = \sqrt{\beta/|\gamma|}$ corresponding to the period of the gap function oscillation in the Fulde-Ferrell-Larkin-Ovchinnikov phase. The Josephson current for $\gamma = 0$ has previously been calculated in Ref. [45]. Here we analyze the case of an arbitrary negative γ restricting ourselves by the condition $\xi_f < \xi = \sqrt{|\gamma|/a}$, meaning the absence of the intrinsic superconductivity in the wire. For simplicity, we also assume that (i) the spin-orbit coupling is weak and can be treated perturbatively, (ii) $L \gg \sqrt{\xi^2 + \xi_f\xi}$, (iii) inside the S leads the Zeeman interaction is negligible, (iv) the conductivity of the S leads well exceeds the one in the wire, so the inverse proximity effect can be neglected, (v) at the S-nanowire interfaces there is no barrier and, thus, the order parameter is continuous at $x = \pm L/2$: $\Psi_n(\pm L/2) = \Delta_n \exp(\pm i\varphi/2)$. Using the boundary conditions, we find the supercurrent $j_x = -c\delta F/\delta A_x$ in the n-th channel [42]: $j_n = j_c^{(n)} \sin[\varphi + (-1)^n \pi\Phi/\Phi_0 + \varphi_0]$, where $\sin\varphi_0 = \sinh(sL)\cos\chi/\sqrt{\sin^2\chi + \sinh^2(sL)}$,

$$j_c^{(n)} = \frac{16|e|\beta\Delta_n^2 k^-}{(\xi_f\xi)^{3/2}k^+} e^{-k^- L}\sqrt{\sin^2\chi + \sinh^2(sL)}, \quad (12)$$

$\sin(\chi - k^+L) = k^+(\xi_f - 2\xi)\sqrt{\xi/\xi_f}$, $s = \nu H/(4\beta k^+k^-)$, and $k^\pm = \xi^{-1}\sqrt{(\xi/\xi_f \pm 1)/2}$.

Summing up the contributions from both channels, we find the magnetic field dependence of the critical current demonstrating the multiperiodic magnetic oscillations. The period of the fast oscillations is again equal to Φ_0/LD, while the slow oscillations caused by the Zeeman interaction are determined by the dependence of the coefficient γ on H. For long junctions with $L \sim s^{-1}$, the term $\sinh^2(sL)$ can result in an increase in I_c with increasing H. Obviously, this effect can be suppressed because of a damping of the superconductivity inside the S leads due to the magnetic field. However, for the Pb films and $LaAlO_3/SrTiO_3$ heterostructures with strong spin-orbit coupling in rather small magnetic fields, the increasing dependencies $T_c(H)$ were observed [46]. In this case, as follows from Eq. (12), the dependencies $I_c(H)$ should reveal the increasing trend due to the spin-orbit coupling.

To sum up, we have suggested phenomenological models describing the distinctive features of the very rich interference physics in nanowires coupled to the superconducting leads. These generic models allowed us to demonstrate the crucial role of electron spectrum nonparabolicity for the φ_0-junction formation, to explain the multiperiodic magnetic oscillations in the Josephson transport through Bi nanowires [20], and also to predict the fundamental period doubling for the SQUID-like critical current oscillations. The discovered phenomena are of

current importance for the superconducting electronics since they may open a way for the new generation of Josephson π- and φ_0-junctions in which the current-phase relation can be tuned by the magnetic field.

The authors thank H. Bouchiat, S. Guéron, A. Murani, and J. Cayssol for the stimulating discussions. This work was supported by the French ANR "MASH," NanoSC COST Action MP1201, the Russian Foundation for Basic Research, the Russian Presidential Foundation (Grant No. SP-6340.2013.5), the Russian Ministry of Science and Education Grant No. 02.B.49.21.0003, and Russian Science Foundation (Grant No. 15-12-10020).

[1] X.-L. Qi and S.-C. Zhang, Rev. Mod. Phys. **83**, 1057 (2011).
[2] A. H. Castro Neto, F. Guinea, N. M. R. Peres, K. S. Novoselov, and A. K. Geim, Rev. Mod. Phys. **81**, 109 (2009).
[3] J.-C. Charlier, X. Blase, and S. Roche, Rev. Mod. Phys. **79**, 677 (2007).
[4] V. Mourik, K. Zuo, S. M. Frolov, S. R. Plissard, E. P. A. M. Bakkers, and L. P. Kouwenhoven, Science **336**, 1003 (2012).
[5] A. Nikolaeva, D. Gitsu, L. Konopko, M. J. Graf, and T. E. Huber, Phys. Rev. B **77**, 075332 (2008).
[6] H. O. H. Churchill, V. Fatemi, K. Grove-Rasmussen, M. T. Deng, P. Caroff, H. Q. Xu, and C. M. Marcus, Phys. Rev. B **87**, 241401(R) (2013).
[7] A. I. Buzdin, Rev. Mod. Phys. **77**, 935 (2005).
[8] A. Buzdin, Phys. Rev. Lett. **101**, 107005 (2008).
[9] J. Alicea, Rep. Prog. Phys. **75**, 076501 (2012).
[10] A. Das, Y. Ronen, Y. Most, Y. Oreg, M. Heiblum, and H. Shtrikman, Nat. Phys. **8**, 887 (2012).
[11] E. J. H. Lee, X. Jiang, R. Aguado, G. Katsaros, C. M. Lieber, and S. De Franceschi, Phys. Rev. Lett. **109**, 186802 (2012).
[12] J. Cayssol, T. Kontos, and G. Montambaux, Phys. Rev. B **67**, 184508 (2003).
[13] A. A. Reynoso, G. Usaj, C. A. Balseiro, D. Feinberg, and M. Avignon, Phys. Rev. Lett. **101**, 107001 (2008).
[14] I. V. Krive, A. M. Kadigrobov, R. I. Shekhter, and M. Jonson, Phys. Rev. B **71**, 214516 (2005).
[15] Y. Tanaka, T. Yokoyama, and N. Nagaosa, Phys. Rev. Lett. **103**, 107002 (2009).
[16] J.-F. Liu and K. S. Chan, Phys. Rev. B **82**, 125305 (2010).
[17] M. Cheng and R. M. Lutchyn, Phys. Rev. B **86**, 134522 (2012).
[18] A. Brunetti, A. Zazunov, A. Kundu, and R. Egger, Phys. Rev. B **88**, 144515 (2013).
[19] T. Yokoyama, M. Eto, and Yu. V. Nazarov, Phys. Rev. B **89**, 195407 (2014); T. Yokoyama, M. Eto, and Yu. V. Nazarov, arXiv:1408.0194.
[20] C. Li, A. Kasumov, A. Murani, S. Sengupta, F. Fortuna, K. Napolskii, D. Koshkodaev, G. Tsirlina, Y. Kasumov, I. Khodos, R. Deblock, M. Ferrier, S. Guéron, and H. Bouchiat, Phys. Rev. B **90**, 245427 (2014).
[21] Yu. M. Koroteev, G. Bihlmayer, J. E. Gayone, E. V. Chulkov, S. Blugel, P. M. Echenique, and Ph. Hofmann, Phys. Rev. Lett. **93**, 046403 (2004).
[22] T. Hirahara, K. Miyamoto, I. Matsuda, T. Kadono, A. Kimura, T. Nagao, G. Bihlmayer, E. V. Chulkov, S. Qiao, K. Shimada, H. Namatame, M. Taniguchi, and S. Hasegawa, Phys. Rev. B **76**, 153305 (2007).
[23] B. Seradjeh, J. Wu, and P. Phillips, Phys. Rev. Lett. **103**, 136803 (2009).
[24] P. Hofmann, Prog. Surf. Sci. **81**, 191 (2006).
[25] C. W. J. Beenakker, Phys. Rev. Lett. **67**, 3836 (1991).
[26] E. I. Rashba, Fiz. Tverd. Tela (Leningrad) **2**, 1224 (1960) [Sov. Phys. Solid State **2**, 1109 (1960)]; Yu. A. Bychkov and E. I. Rashba, Pis'ma Zh. Eksp. Teor. Fiz. **39**, 66 (1984) [JETP Lett. **39**, 78 (1984)].
[27] R. M. Lutchyn, J. D. Sau, and S. Das Sarma, Phys. Rev. Lett. **105**, 077001 (2010).
[28] Y. Oreg, G. Refael, and F. von Oppen, Phys. Rev. Lett. **105**, 177002 (2010).
[29] T. D. Stanescu, R. M. Lutchyn, and S. Das Sarma, Phys. Rev. B **84**, 144522 (2011).
[30] The straightforward derivation of Eq. (5) for $u^{\pm}_{n\downarrow}$, $v^{\pm}_{n\uparrow}$, and $v^{\pm}_{n\downarrow}$ gives $\mp iv_F^{\mp}\partial_x\tilde{u}^{\pm}_{n\downarrow} = \varepsilon\tilde{u}^{\pm}_{n\downarrow}$, $\mp iv_F^{\mp}\partial_x\tilde{v}^{\pm}_{n\uparrow} = -\varepsilon\tilde{v}^{\pm}_{n\uparrow}$, and $\mp iv_F^{\pm}\partial_x\tilde{v}^{\pm}_{n\downarrow} = -\varepsilon\tilde{v}^{\pm}_{n\downarrow}$.
[31] E. V. Bezuglyi, A. S. Rozhavsky, I. D. Vagner, and P. Wyder, Phys. Rev. B **66**, 052508 (2002); L. DellAnna, A. Zazunov, R. Egger, and T. Martin, Phys. Rev. B **75**, 085305 (2007).
[32] A. Zazunov, R. Egger, T. Jonckheere, and T. Martin, Phys. Rev. Lett. **103**, 147004 (2009).
[33] T. Schäpers, *Superconductor/Semiconductor Junctions*, Springer Tracts on Modern Physics Vol. 174 (Springer-Verlag, Berlin, 2001).
[34] The unitarity condition requires the matrices $\hat{R}^{\pm}_j$ and $\hat{A}^{\pm}_j$ to satisfy the relations $\hat{R}^{\pm}_j\hat{R}^{\pm\dagger}_j + \hat{A}^{\mp}_k\hat{A}^{\mp\dagger}_k = \hat{1}$ and $\hat{R}^{\pm}_j\hat{A}^{\pm\dagger}_j + \hat{A}^{\mp}_k\hat{R}^{\mp\dagger}_k = \hat{0}$, where $j,k \in \{e,h\}$ and $j \neq k$.
[35] The accurate microscopical calculations of the induced gap values Δ_n can be performed in the spirit of Refs. [36–39]. However, such calculations cannot influence the results of our paper since, for small tunneling rates between the conductive channels and the S leads, the exact gap functions Δ_n are just some energy-independent constants.
[36] A. F. Volkov, P. H. C. Magnée, B. J. van Wees, and T. M. Klapwijk, Physica C (Amsterdam) **242**, 261 (1995).
[37] G. Fagas, G. Tkachov, A. Pfund, and K. Richter, Phys. Rev. B **71**, 224510 (2005).
[38] J. D. Sau, R. M. Lutchyn, S. Tewari, and S. Das Sarma, Phys. Rev. B **82**, 094522 (2010).
[39] N. B. Kopnin and A. S. Melnikov, Phys. Rev. B **84**, 064524 (2011).
[40] N. B. Kopnin, A. S. Melnikov, V. I. Pozdnyakova, D. A. Ryzhov, I. A. Shereshevskii, and V. M. Vinokur, Phys. Rev. Lett. **95**, 197002 (2005).
[41] J. Demers and A. Griffin, Can. J. Phys. **49**, 285 (1971).
[42] See Supplemental Material at http://link.aps.org/supplemental/10.1103/PhysRevLett.114.227001 for a detailed calculation of the critical current within the BdG and Ginzburg-Landau formalisms.
[43] K. V. Samokhin, Phys. Rev. B **70**, 104521 (2004).
[44] R. P. Kaur, D. F. Agterberg, and M. Sigrist, Phys. Rev. Lett. **94**, 137002 (2005).
[45] A. I. Buzdin and M. L. Kulić, J. Low Temp. Phys. **54**, 203 (1984).
[46] H. J. Gardner, A. Kumar, L. Yu, P. Xiong, M. P. Warusawithana, L. Wang, O. Vafek, and D. G. Schlom, Nat. Phys. **7**, 895 (2011).